EURASIAN PHYSICAL TECHNICAL JOURNAL

2024, Volume 21, No. 2 (48)

https://doi.org/10.31489/2024No2/92-101

Received: 07/04/2024 Revised: 17/04/2024 Accepted: 18/06/2024 Published online: 29/06/2024

Original Research Article

UDC: 53.03; 524.7, 524-1:629.78

FINITE TEMPERATURE EFFECTS WITHIN SCALAR FIELD DARK MATTER MODEL

Suliyeva G.B.[1,2,3], Kurmanov Ye.B.[1,2,4], Konysbayev T.K.[1,2], Boshkayev K.A.[1,2,5], Urazalina A.A.[1,2,5], Luongo O.[2,6,7,8,9]

[1] National Nanotechnology Laboratory of Open Type, Almaty, Kazakhstan
[2] Al-Farabi Kazakh National University, Almaty, Kazakhstan
[3] Fesenkov Astrophysical Institute, Almaty, Kazakhstan
[4] International Engineering Technological University, Almaty, Kazakhstan
[5] Institute of Nuclear Physics, Almaty, Kazakhstan
[6] Università di Camerino, Camerino, Italy
[7] SUNY Polytechnic Institute, New York, USA
[8] INAF – Osservatorio Astronomico di Brera, Milano, Italy
[9] Instituto Nazionale di Fisica Nucleare, Perugia, Italy
*Corresponding author: kurmanov.yergali@kaznu.kz

Abstract. *The distribution of dark matter in four low surface brightness spiral galaxies is studied using two models within the scalar field theory of dark matter, an alternative to the cold dark matter paradigm. The first model is a Bose-Einstein condensate, in which bosons occupy the ground state at zero temperature. The second model includes finite temperature corrections to the scalar field potential, which allows the introduction of excited states. A nonlinear least squares approximation method is used to determine the free parameters of the models, including scale radius, characteristic (central) density and total mass, based on observational data of rotation curves. Quantitative analysis shows the importance of considering finite temperatures at the galactic level. In addition, the two models are compared with results from widely used and accepted phenomenological dark matter profiles such as the isothermal sphere, Navarro-Frank-White and Burkert profiles. The reliability of each model was assessed based on the Bayesian information criterion of completeness. Statistical analysis provides meaningful interpretation of the choice of a particular profile. Ultimately, this study contributes to a better understanding of the distribution of dark matter in low surface brightness spiral galaxies by shedding light on the performance of scalar field models compared to traditional phenomenological profiles.*

Keywords: scalar field, dark matter, Bose-Einstein condensate, galaxy rotation curves.

1. Introduction

The presence of dark matter (DM) in the Universe is firmly confirmed by extensive observational data. Initially, the concept of DM emerged as a solution accounting for the rotation curves of spiral galaxies, the velocity dispersions observed within galaxy clusters, and the measured mass-to-light ratios in individual galaxies as well as in clusters of galaxies [1-3]. Afterwards, its importance became increasingly evident in interpreting a variety of astrophysical and cosmological phenomena, such as gravitational lensing, the

presence of acoustic baryonic oscillations, the power spectrum of galaxies, and0 the formation of cosmic structures in the early Universe [4-5]. The widely known model for DM is the Cold Dark Matter (CDM) paradigm which demonstrated remarkable success in reproduction and explanation of many cosmic phenomena on cosmological scales [6-7]. Nevertheless, it encounters several notable challenges and shortcomings when applied to the galactic and sub-galactic levels [8].

Namely, among them:

– the cusp-core problem, arising as CDM model predicts that DM halos should have a density profile with a central "cusp" (a steep increase in density toward the center), whereas observations of galaxies often suggest a "core" (a relatively flat density profile);

– the redundant presence of substructures as predicted by N-body numerical simulations, which significantly exceed the observed values.

There exist different candidates for DM, but in this work, we will examine the Scalar Field Dark Matter (SFDM) as this model provides a naturally emerging solution to the CDM problems mentioned above. Unlike many other DM models that require the existence of new particles or forces beyond those in the Standard Model of particle physics, SFDM relies on a simple and elegant concept – a scalar field (SF).

The central idea suggesting that dark matter is a spin-0 SF forming Bose-Einstein condensate (BEC) "drops" was first considered in [9] and independently in [10-12]. Indeed, this model may admit various specific properties studied by different authors. In the literature, it is also appeared as fuzzy DM [13], wave DM [14], Bose-Einstein condensate DM [15]. In the framework of SFDM, it is possible to account for temperatures (see Sec. 1). In the present paper, we focus on manifestation of SFDM properties on galactic level. The issue of dark matter distribution in galaxies is primarily concerned with halo regions and is linked to the rotation curves (RC) of galaxies obtained from observations. The aim of this work is to explore the consistency of the two SFDM models by comparing the rotation curves of four representative Low Surface Brightness spiral galaxies without involving the baryonic component and taking into account the internal galaxies' structure. To achieve this, we perform nonlinear fitting procedure and employ a statistical tool - the Bayesian Information Criterion (BIC) to estimate the goodness of the fit.

On the other hand, for comparison we consider well-corroborated phenomenological profiles, which are widely exploited in the literature: Navarro-Frenk-White (NFW), Burkert profiles and Isothermal sphere (ISO). These profiles have been proposed as parametrized functions that can fit numerical simulations and observations fairly well, regardless the underlying theories or theoretical motivation. The model parameters for each of these profiles are the scale radius r_0 and the DM density at galaxy center ρ_0.

The article is organized as follows. In Sec. 2, we describe the features of two specified SFDM models. In Sec. 3, the methods necessary for carrying the fitting procedure are presented. Sec. 4 introduces the major results of the paper. In Sec. 5, conclusion remarks are reported.

2. Dark matter models: fundamental and phenomenological

2.1 Haloes at zero-temperatures

Bosons at zero temperature are studied in many works. Since almost all bosons occupy the ground state at temperatures close to absolute zero, the behavior of the haloes can be effectively described using the principles of Bose-Einstein condensation (BEC). Employing the Bogolyubov approximation [16], which is a method commonly used in the study of quantum systems, allows for a classical mean-field representation of the ground state of the SFDM haloes. This approach simplifies the analysis by neglecting the contribution of excited states, thereby focusing solely on the dominant ground state configurations.

Bohmer and Harko [15] utilized the Thomas-Fermi limit, where the self-interactions of the SF play a prominent role in the SFDM potential. This limit simplifies the analysis by allowing the mass term $\sim \Phi^2$ to be disregarded and the potential is expressed in the form $V(\Phi) \sim \lambda\Phi^4$, where λ is the coupling constant. Using this limit, the authors derived the solution of equation describing the single static BEC:

$$\nabla^2\rho(r) + k^2\rho(r) = 0, \tag{1}$$

where $\rho(r)$ is the DM density distribution, k is the parameter. The solution is:

$$\rho(r) = \rho_0 \frac{\sin(kr)}{kr}, \tag{2}$$

with $\rho_0 = \rho(0)$ being the central density. The above solution has a condition for a bound halo radius R given by $\rho(R) = 0$ in order to obviate non-physical negative densities. Hence, one gets $k = \pi / R$. The radius of the BEC halo is given by expression:

$$R = \pi \sqrt{\frac{\hbar^2 a}{Gm^3}}, \tag{3}$$

consisting of fixed values, where $\hbar$ is the reduced Plank's constant, G is the gravitational constant, m is the boson's mass, a is the scattering length. Eq. (3) is linked to the coupling constant via $\lambda = 4\pi\hbar^2 a / m$.

2.2 Finite-temperature haloes

The study [17] introduced a scenario where the scalar field (SF) operates under conditions of finite temperature. The authors considered a self-interacting spin-0 real SF immersed in a thermal bath (i.e. a medium or reservoir of particles that are in thermal equilibrium) at temperature T. The SF potential is written in the following form [18]:

$$V(\Phi) = -\frac{1}{2}m^2\Phi^2 + \frac{1}{4}\lambda\Phi^4 + \frac{1}{8}\lambda\Phi^2T^2 - \frac{\pi^2}{90}T^4, \tag{4}$$

in the units where the speed of light $c = 1$, the Boltzmann constant $k_B = 1$ and $\hbar = 1$. The first term corresponds to the mass term, the second term represents the repulsive self-interaction, the third term describes the interaction of the field with the thermal bath, and the last term accounts for the influence of the thermal bath alone.

It was shown that early dark matter (DM) haloes were formed after the growth in SF fluctuations occurring after the spontaneous symmetry breaking (SSB) of the system [19]. The equilibrium temperatures of these haloes vary depending on when each halo forms.

Since galactic halos are well described by Newtonian dynamics, an exact analytic solution for SF can be found in the limit of weak gravitational field regime. Finally, the analytical solution, in the weak field regime, is presented as a linear combination:

$$\rho(r) = \sum_j \rho_0^j \left[\frac{\sin(k_j r)}{k_j r}\right]^2, \tag{5}$$

where $j = 1, 2, 3, \ldots$ is the number of exited states, required to fit the distribution; $\rho_0^j = \rho^j(0)$ is the central density of a single state, and the scale of the SF configuration is determined due to the condition $\rho^j(R) = 0$, i.e. $k_j R = j\pi$. This density has a naturally occurring core. Consequently, the overall solution allows for a configuration beyond a completely condensed system, and the potential adjusted for finite temperature suggests the presence of separate excitation states j as solutions to the perturbation equation of the SF. This indicates that the bosons are distributed thermally among both ground and excited states at higher energy levels.

2.3 Phenomenological models

Here we review some basic models widely exploited in the literature.

The NFW profile [20] was introduced after stacking numerous halos in order to fit the data of N-body simulations within the CDM model. It is given by

$$\rho(r) = \frac{\rho_0}{(r/r_0)(1 + r/r_0)^2}. \tag{6}$$

The Burkert profile [21] which firstly was proposed in the attempt to determine the density law that best fit the measured rotation curves of dwarf galaxies, which are known to be dominated by DM, has the following form:

$$\rho(r) = \frac{\rho_0}{(1 + r/r_0)(1 + (r/r_0)^2)}. \tag{7}$$

The ISO profile [22] has been employed in the context of galactic dynamics, particularly in explaining the flat rotation curves observed in spiral galaxies. It is expressed as:

$$\rho(r) = \frac{\rho_0}{1+(r/r_0)^2}. \tag{8}$$

These models along with the two SF models will be employed to analyze DM distribution in the LSB galaxies.

3. Methods

The galaxy RC is a measure of how the rotational velocity of objects in a galaxy changes with their distance from the galactic center. Since the Newtonian dynamics is sufficient at the galactic level, rotational velocity $V(r)$ is represented by:

$$V(r) = \sqrt{r\frac{\partial\phi}{\partial r}} = \sqrt{\frac{GM(r)}{r}}, \tag{9}$$

where $\phi(r)$ is the gravitational potential corresponding to the mass distribution $M(r)$. Each profile generates a particular RC and hence yields corresponding DM mass distributions that can be calculated by integration of density:

$$M(r) = 4\pi\int_0^r r'^2\rho(r')dr'. \tag{10}$$

Thereby, taking Eqs. (2) and (5) one obtains the mass profile

$$M(r) = \frac{4\pi\rho_0 r}{k^2}\left(\frac{\sin(kr)}{kr} - \cos(kr)\right), \tag{11}$$

for haloes with zero temperatures, and

$$M(r) = \sum_j M_j = \sum_j \frac{2\pi\rho_0 r}{k_j^2}\left(1 - \frac{\sin(2k_j r)}{2k_j r}\right), \tag{12}$$

for finite temperatures haloes with M_j being the total mass of state j.

It should be noted, that in numerical computations/analyses the mass is expressed in the units of solar mass ($M_\odot$) and the radial distance is in kilo-parsecs (kpc).

After establishing the mass and velocity profiles, the next step is to perform fitting procedure. In this work, we employ the Levenberg-Marquardt nonlinear least squares method [23-24]. The calibration is based on observational data including measurements of radial velocity. After that, an objective function χ^2 representing the squared differences between observed V_l^{obs} and expected $V(r)$ velocities describing each profile is created:

$$\chi^2 = \sum_{l=1}^{N}\left[\frac{V_l^{obs} - V(r)}{\sigma_{V,l}^{obs}}\right]^2, \tag{13}$$

where N is the number of data points, $\sigma_{V,l}^{obs}$ is their corresponding errors. The key to the approach is to minimize this objective function by iteratively modifying the model parameters. This will guarantee the best possible fit, since the process systematically reduces the discrepancies between the model and the observed data, leading to an accurate and reliable representation of the galaxy's RC. The "best fit" in this context means that the model parameters have been chosen such that the divergence between the observed data and the model's predictions is minimized.

In this context, models fitted to the same data set can be compared quantitatively using the Bayesian Information Criterion (BIC):

$$\mathrm{BIC} = \chi^2 + p\ln N, \tag{14}$$

where p is the number of free model parameters. A better trade-off between model fit and simplicity is demonstrated by lower BIC values increasing the benefits of the model.

4. Results

In this section we present the results of fitting procedure for 4 LSB spiral galaxies - NGC 1560, NGC 1003, NGC 3741, NGC 6503, the observational data points of which are taken from the SPARC database (Spitzer Photometry and Accurate Rotation Curves) [25]. In comparison to high surface brightness galaxies, LSB galaxies are thought to contain a higher proportion of DM relative to visible matter. This fact allows one to neglect the baryonic component in the galaxy structure and adopt the total mass M_{tot} approximately equal to the DM mass M_{DM} ($M_{tot} \approx M_{DM}$).

Primarily, we compare two SFDM models, declared by Eqs. (2) and (5), to estimate quantitatively how the influence of finite temperature effects affects the consistency of the models with the observations. In the case of the BEC SFDM profile, fitting analysis provides two free parameters: the halo radius R and the central density ρ_0, imposing the ground state only ($j=1$). At the same time, for the mSFDM model three free parameters are required: as we take two states, the central density of each state should be ensured (finally, we have R, ρ_0^i, ρ_0^j). It is worth mentioning, that the combination of states (i, j) differs from one galaxy to another and is selected manually until the best correspondence with observations is achieved. The numerical outcomes are presented in Table 1 and in Fig. 1.

Table 1. Fitting parameters for 4 LSB galaxies within the SFDM models.

Profile	i, j	R, kpc	ρ_0^i, $10^{-3}\frac{M_\odot}{pc^3}$	ρ_0^j, $10^{-3}\frac{M_\odot}{pc^3}$	M_{tot}, $10^{10}M_\odot$	$<\rho>$, $10^{-3}\frac{M_\odot}{pc^3}$	BIC	ΔBIC
NGC 1560								
BEC SFDM	1	8.37	23.36	-	0.87	3.52	199.9	80.0
mSFDM	1, 3	12.46	8.86	33.88	1.04	1.28	119.9	-
NGC 1003								
BEC SFDM	1	15.15	16.03	-	7.08	4.87	195.3	124.7
mSFDM	1, 4	42.91	0.79	24.69	8.27	0.25	70.6	-
NGC 3741								
BEC SFDM	1	6.66	16.88	-	0.33	2.69	105.8	60.5
mSFDM	1, 6	8.69	7.97	85.44	0.35	1.27	45.3	-
NGC 6503								
BEC SFDM	1	5.68	15.47	-	7.30	9.53	161.9	45.0
mSFDM	1, 3	13.70	26.74	964.65	7.41	6.87	116.9	-

For both models, the total mass M_{tot} is computed using the last data point of the distance by substituting the fitting parameters into the Eqs. (11) and (12). The average density $<\rho>$ is obtained through the standard density definition, dividing the total mass M_{tot} by the volume enclosed within the corresponding distance. It should be noted, that a third (forth, and so on) exited state might be added to the analysis, however it is not necessary, as the introduction of only two states is enough for the whole procedure.

As mentioned before, the model that has the lowest BIC, say BIC_0, is regarded as the best-suited model. When compared to other models, the difference $\Delta BIC = BIC - BIC_0$ certifies the statistical evidence supporting the reference model as the best-fitting one. In particular, the case $\Delta BIC \in [0,2]$ shows a weak evidence, the case $\Delta BIC \in [3,6]$ shows a mild evidence, and the case $\Delta BIC > 6$ shows a strong evidence.

For all considered galaxies, mSFDM model demonstrates lower values of BIC, indicating that this model is more suitable to represent DM. Moreover, from Fig. 1 one can see that RCs for mSFDM model reveal better concordance with observational data in comparison to BEC SFDM. Notably, for one galaxy (NGC 6503), the best fit is reached with two exited states only ($i=2$, $j=7$), while for the rest galaxies (NGC 1560, NGC 1003, NGC 3741) the ground state ($j=1$) is present. In addition to SFDM models, we

carried out the fitting procedure for phenomenological profiles: NFW, Burkert and ISO to assess the contrast between them and to be convinced whether mSFDM is a reliable alternative for DM representation.

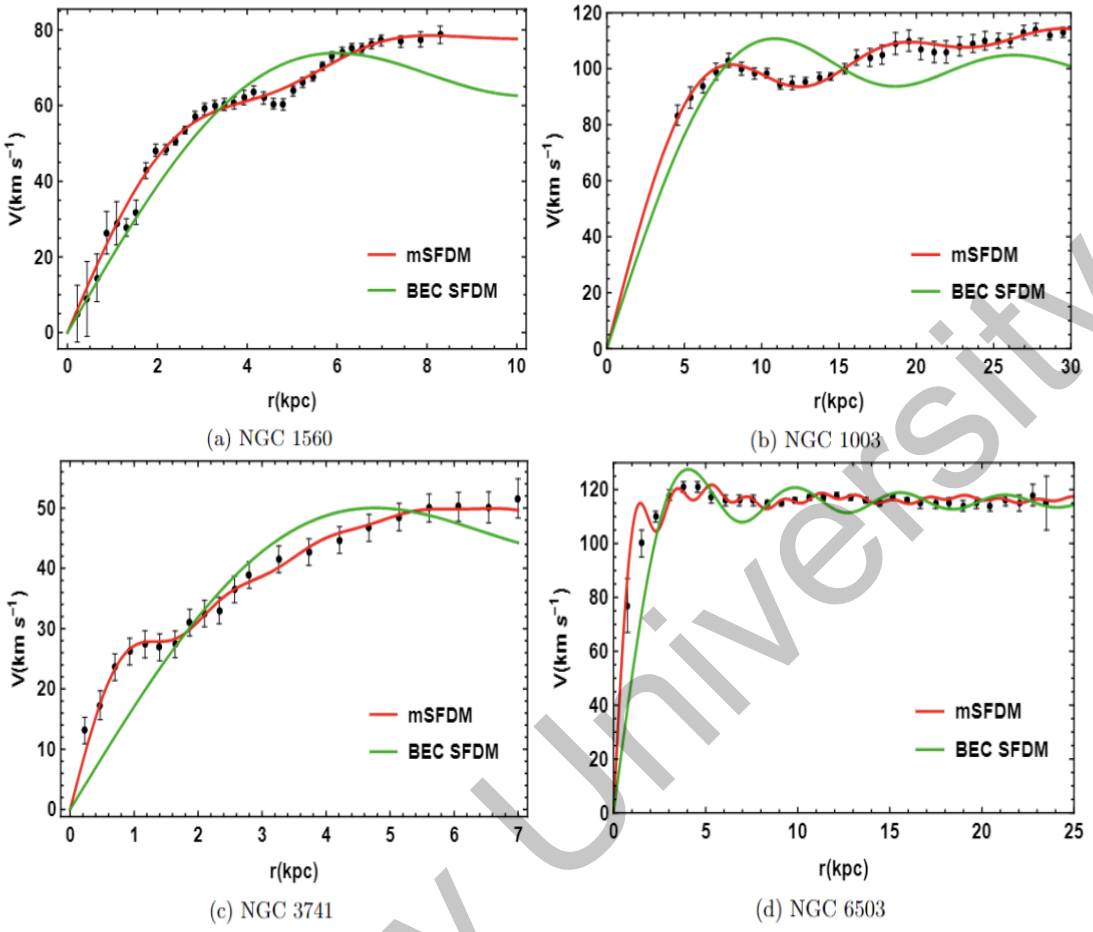

Fig.1. Rotation curves of LSB galaxies for the two SFDM models: black dots represent the observational data with their error bars, the green solid curve corresponds to the BEC SFDM, the red solid curve - to the mSFDM

In Table 2, the fitting parameters (scale radius r_0 and central (characteristic) density ρ_0) are shown. The total mass M_{tot} and the average density $<\rho>$ are calculated in the same way as in the Table 1. Note, that here values of ΔBIC are calculated with respect to mSFDM being the reference model with BIC=BIC$_0$ = [119.9, 70.6, 45.3, 116.9] for NGC 1560, NGC 1003, NGC 3751, NGC 6503 galaxies, correspondingly. When comparing the values of BIC in Tables 2 and 1, it is clearly seen that, in cases of all considered galaxies, they consistently emerge as the lowest for mSFDM model.

Values of ΔBIC demonstrate strong evidence for mSFDM model to be preferable over phenomenological models with two exceptions: for NGC 3741 NFW profile yields ΔBIC=5.7, indicating the mild evidence, and for NGC 6503 ISO profile gives ΔBIC=0.5, implying that it provides fit as well as mSFDM. Meanwhile, for NGC 1560, NGC 1003 and NGC 1560 the phenomenological models display lower BIC values in comparison to BEC SFDM. However, for NGC 6503 the highest BIC shows the Burkert profile. This emphasizes the importance of the choice of DM model to the specific characteristics of each galaxy, as different systems may demand different representations of DM distribution.

Based on graphical representation of fitting results (Fig.2), mSFDM model is able to reproduce the wiggles in observed RCs, in contrast to phenomenological ones. This possibility is crucial for understanding the dynamics of galaxies and provides a significant advantage to mSFDM model.

Table 2. Fitting parameters for 4 LSB galaxies within the phenomenological models.

Profile	r_0, kpc	ρ_0, $10^{-3}\frac{M_\odot}{pc^3}$	M_{tot}, $10^{10}M_\odot$	$<\rho>$, $10^{-6}\frac{M_\odot}{pc^3}$	BIC	ΔBIC
NGC 1560						
NFW	21.06	2.12	0.12	5.19	151.2	31.3
Burkert	3.23	4.73	0.01	0.59	159.2	39.3
ISO	1.84	4.61	1.63	68.3	150.9	31.0
NGC 1003						
NFW	15.11	4.55	0.13	0.12	151.3	80.7
Burkert	6.58	23.35	0.06	5.52	173.9	103.3
ISO	2.07	57.99	9.41	8.12	145.5	74.9
NGC 3741						
NFW	15.17	1.52	0.04	2.63	51.0	5.7
Burkert	2.29	37.49	0.004	0.29	88.5	43.2
ISO	1.15	43.16	0.51	3.52	83.9	38.6
NGC 6503						
NFW	3.57	95.82	0.04	7.86	145.8	28.9
Burkert	2.09	296.16	0.03	5.33	174.6	57.7
ISO	0.16	98.68	7.56	13.9	117.4	0.5

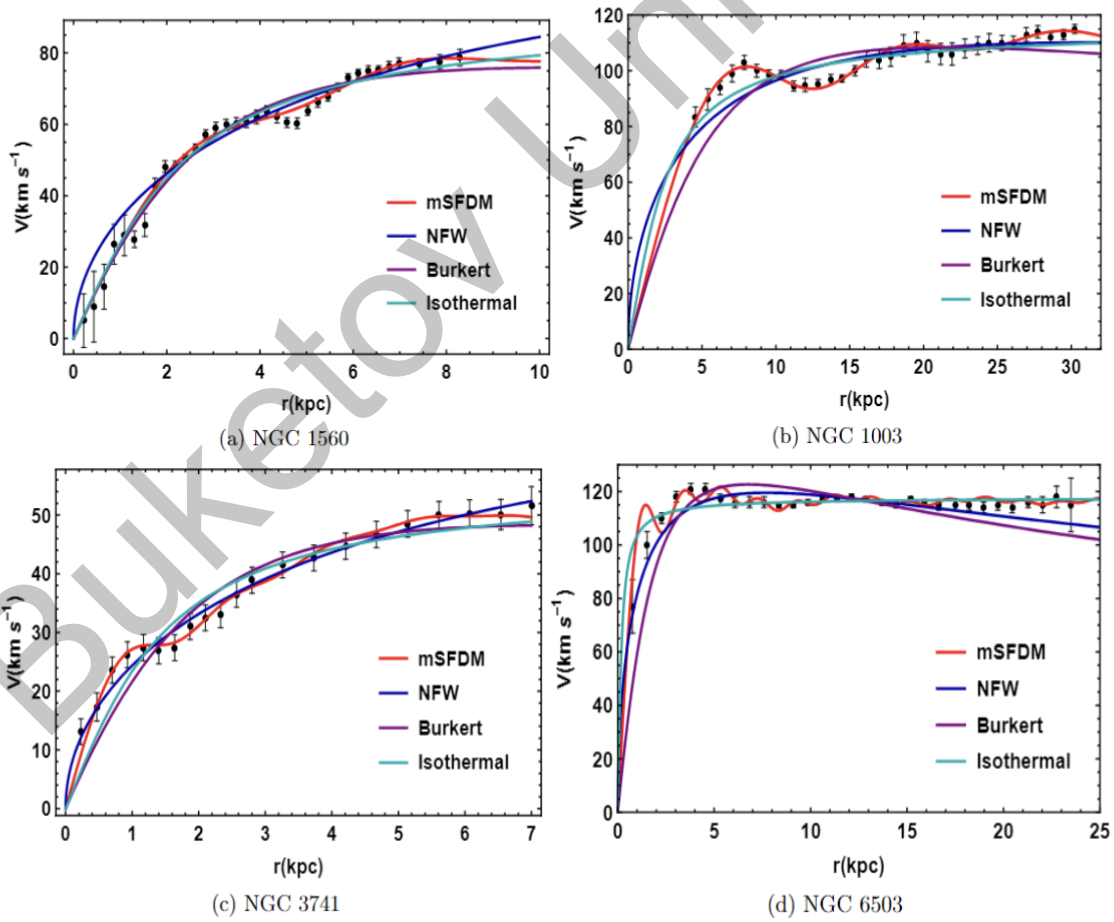

(a) NGC 1560 (b) NGC 1003

(c) NGC 3741 (d) NGC 6503

Fig.2. Rotation curves of LSB galaxies for mSFDM and three phenomenological (NFW, Burkert, ISO) models

5. Conclusion

In this work, we have analyzed four LSB spiral galaxies (range of sizes $\sim 7-30$ kpc) within the framework of two SFDM models regardless of the impact of baryonic component and internal structure of galaxies. First one, the so-called BEC SFDM, implies the system of bosons in the ground state and at zero-temperature in the Thomas-Fermi limit. Second one, mSFDM, is the model with finite temperature corrections which lead to taking into consideration exited states of bosons. We performed the fitting procedure to constrain the free models' parameters and to estimate which model is more preferable and consistent with observations. The mSFDM with lower values of BIC for all considered galaxies proved to be better representation model for DM. To further verify the appropriateness of mSFDM model, we compared it with NFW, Burkert and ISO profiles as representative examples of phenomenological framework. For each galaxy, mSFDM provides better results keeping the lowest values of BIC and showing the excellent agreement with observations. The mSFDM model incorporates finite temperature effects and allows for multistate occupation of bosons, which are particularly relevant in scenarios where thermal effects cannot be ignored. This is expected to be the case in certain early-universe conditions or in environments with significant thermal history affecting dark matter distribution.

Within this article, we did not conduct a detailed analysis and comparison between phenomenological models themselves, since related work was done in several papers (see, for example, [26-30]).

Nevertheless, in case of NGC 1560 and NGC 6503 there are some data points not covered even by mSFDM, suggesting the need for further analysis. An additional numerical analysis is required to examine the influence of baryonic matter as well as including into consideration the inner structure of galaxies. Besides, more galaxies should be analyzed, to estimate the degree of applicability mSFDM model within the wide range of galaxies. Moreover, it would be interesting to examine the SFDM models in Milky Way and Andromeda galaxies, following the methodology described in [31-33].

Conflict of interest statement

The authors declare that they have no conflict of interest in relation to this research, whether financial, personal, authorship or otherwise, that could affect the research and its results presented in this paper.

CRediT author statement

Suliyeva G.B.: Conceptualization, Writing -Original Draft; Kurmanov Ye.B.: Writing -Review & Editing; Konysbayev T.K.: Software; Boshkayev K.A.: Methodology, Supervision; Urazalina A.A.: Investigation; Luongo O.: Validation
The final manuscript was read and approved by all authors.

Acknowledgments

Suliyeva G.B., Kurmanov Ye.B. acknowledge Grant No. AP23488743, AP19575366;
Konysbayev T.K. acknowledges the Grant No. AP19174979;
Boshkayev K.A., Luongo O. acknowledge Grant No. AP19680128;
Urazalina A.A. acknowledges Grant No. BR21881941 from the Science Committee
of the Ministry of Science and Higher Education of the Republic of Kazakhstan.

References

1 Zwicky F. (1933) Die rotverschiebung von extragalaktischen nebeln. *Helvetica Physica Acta*. 6, 110-127. Available at: https://ned.ipac.caltech.edu/level5/March17/Zwicky/frames.html

2 Rubin V.C., Ford Jr.W. K., Thonnard N. (1980) Rotational properties of 21 SC galaxies with a large range of luminosities and radii, from NGC 4605/R= 4kpc/to UGC 2885/R= 122 kpc. *Astrophysical Journal*. 238, 471- 487. Available at: https://articles.adsabs.harvard.edu/pdf/1980ApJ...238..471R

3 Rubin V.C. (1983) The rotation of spiral galaxies. *Science*. 220, 4604, 1339-1344, Available at: https://www.science.org/doi/10.1126/science.220.4604.1339

4 Bertone G., Hooper D., Silk J. (2005) Particle dark matter: Evidence, candidates and constraints. *Physics reports*. 405, 5-6, 279-390. DOI:10.1016/j.physrep.2004.08.031.

5 Bennett C.L., Larson D., Weiland J.L., Jarosik N., Hinshaw G., Odegard N., Smith K.M., Hill R.S., Gold B., Halpern M., Komatsu E., Nolta M.R., Page L., Spergel D.N, Wollack E., Dunkley J., Kogut A., Limon M., Meyer S.S., Tucker G.S., Wright E.L. (2013) Nine-year Wilkinson Microwave Anisotropy Probe (WMAP) observations: final maps

and results. *The Astrophysical Journal Supplement Series*. 208, 2, 1-54. Available at: https://iopscience.iop.org/article/10.1088/0067-0049/208/2/20

6 Benson A.J. (2010) Galaxy formation theory. *Physics Reports*. 495, 2-3, 33-86. DOI:10.1016/j.physrep.2010.06.001.

7 Larson D., Dunkley J., Hinshaw G., Komatsu E., Nolta M.R., Bennett C.L., Gold B., Halpern M., Hill R.S., Jarosik N., Kogut A., Limon M., Meyer S.S., Odegard N., Page L., Smith K.M., Spergel D.N., Tucker G.S., Weiland J.L., Wollack E. and Wright E.L. (2011) Seven-year wilkinson microwave anisotropy probe (WMAP*) observations: power spectra and WMAP-derived parameters. *The Astrophysical Journal Supplement Series*. 192(2), 1-19. DOI:10.1088/0067-0049/192/2/16.

8 Weinberg D.H., Bullock J.S., Governato F., Kuzio de Naray R., Peter H.G. (2015) Cold dark matter: controversies on small scales. *Proceedings of the National Academy of Sciences*. 112, 40, 12249-12255. DOI:10.1073/pnas.1308716112.

9 Ji S.U., Sin S.J. (1994) Late-time phase transition and the galactic halo as a Bose liquid. II. The effect of visible matter. *Physical Review D*. 50, 6, 3655-3659. DOI:10.1103/PhysRevD.50.3655.

10 Guzmán F.S., Matos T. (2000) Scalar fields as dark matter in spiral galaxies. *Classical and Quantum Gravity*. 17 (1) L9-L16. DOI:10.1088/0264-9381/17/1/102.

11 Guzman F.S., Matos T., Villegas H.B. (1999) Scalar fields as dark matter in spiral galaxies: comparison with experiments. *Astronomische Nachrichten: News in Astronomy and Astrophysics*. 320, 3, 97-104. DOI:10.1002/1521-3994(199907)320:3<97::AID-ASNA97>3.0.CO;2-M.

12 Lee J., Koh I. (1996) Galactic halos as boson stars. *Physical Review D*. 53, 4, 2236-2239. DOI:10.1103/PhysRevD.53.2236.

13 Hu W., Barkana R., Gruzinov A. (2000) Fuzzy cold dark matter: the wave properties of ultralight particles. *Physical Review Letters*. 85, 6, 1158-1161. DOI:10.1103/PhysRevLett.85.1158.

14 Schive H.Y., Chiueh T., Broadhurst T. (2014) Cosmic structure as the quantum interference of a coherent dark wave. *Nature Physics*. 10, 7, 496-499. DOI:10.1038/nphys2996.

15 Boehmer C.G., Harko T. (2007) Can dark matter be a Bose–Einstein condensate? *Journal of Cosmology and Astroparticle Physics*. 06, 1-27. DOI:10.1088/1475-7516/2007/06/025.

16 Bogoliubov N. (1947) On the theory of superfluidity. *J. Phys*. 11 (1), 23. Available at: https://inspirehep.net/literature/45477

17 Robles V.H., Matos T. (2012) Exact solution to finite temperature SFDM: natural cores without feedback. *The Astrophysical Journal*. 763, 1, 1-8. DOI:10.1088/0004-637X/763/1/19.

18 Kolb E.W., Turner M.S. (1981) The early universe. *Nature*. 294, 5841, 521-526. DOI:10.1038/294521a0.

19 Castellanos E., Matos T. (2013) Klein–Gordon Fields and Bose–Einstein Condensates: Thermal Bath Contributions. *International Journal of Modern Physics B*. 27, 11, p. 1350060. DOI:10.1142/S0217979213500604.

20 Navarro J.F. (1996) The structure of cold dark matter halos. *Symposium-international astronomical union*. 171, 255-258. DOI:10.48550/arXiv.astro-ph/9511016.

21 Burkert A. (1995) The structure of dark matter halos in dwarf galaxies. *The Astrophysical Journal*. 447, 1, L25-L28. DOI:10.1086/309560.

22 Jimenez R., Verde L., Oh S.P. (2003) Dark halo properties from rotation curves. *Monthly Notices of the Royal Astronomical Society*. 339, 1, 243-259. DOI:10.1046/j.1365-8711.2003.06165.x.

23 Levenberg K. (1944) A method for the solution of certain non-linear problems in least squares. *Quarterly of applied mathematics*. 2 (2), 164-168. DOI:10.1090/qam/10666.

24 Marquardt D.W. (1963) An algorithm for least-squares estimation of nonlinear parameters. *Journal of the society for Industrial and Applied Mathematics*. 11, 2, 431-441. Available at: https://www.jstor.org/stable/2098941.

25 Lelli F., McGaugh S.S., Schombert J.M. (2016) SPARC: Mass models for 175 disk galaxies with Spitzer photometry and accurate rotation curves. *The Astronomical Journal*. 152, 6, 1-14. DOI:10.3847/0004-6256/152/6/157.

26 Kurmanov Ye., Boshkayev K., Konysbayev T., Muccino M., Urazalina A., Ikhsan G., Saiyp N., Rabigulova G, Karlinova M., Suliyeva G., Taukenova A. and Beissen N. (2023) Analysis of dark matter profiles in the halos of spiral galaxies. *Physical Sciences and Technology*. 10, 3-4, 4-16. DOI:10.26577/phst.2023.v10.i2.01.

27 Boshkayev K., Konysbayev T., Kurmanov E., Muccino M. (2020) Dark matter properties in galaxy U5750. *News of the National Academy of Sciences of the Republic of Kazakhstan physico-mathematical series*. 6, 81-90. DOI:10.32014/2020.2518-1726.101.

28 Boshkayev K., Konysbayev T., Kurmanov E., Muccino M., Zhumakhanova G. (2020) Physical properties of dark matter in galaxy U11454. *Physical sciences and technology*, 7, 11-20. DOI:10.26577/phst.2020.v7.i2.02.

29 Boshkayev K., Konysbayev T., Kurmanov E., Luongo O., Muccino M. (2020) Imprint of pressure on characteristic dark matter profiles: the case of ESO0140040. *Galaxies*. 2020, 74, 1-13. DOI:10.3390/galaxies8040074.

30 Boshkayev K., Zhumakhanova G., Mutalipova K., Muccino M. (2019) Investigation of different dark matter profiles. *News of the National Academy of Sciences of the Republic of Kazakhstan Physical and Mathematical Series*. 6, 328, 25-33. DOI:10.32014/2019.2518-1726.70.

31 Sofue Y. (2015) Dark halos of M 31 and the Milky Way. *Publications of the Astronomical Society of Japan*. 67, 4, 75-84. DOI:10.1093/pasj/psv042.

32 Salucci P. (2019) The distribution of dark matter in galaxies. *The Astronomy and Astrophysics Review*. 27, 1 – 60. DOI:10.1007/s00159-018-0113-1.

33 Boshkayev K., Konysbayev T., Kurmanov Ye., Luongo O., Muccino M., Quevedo H., Zhumakhanova G. (2024) *Numerical analyses of M31 dark matter profiles*. 33, 03-04. DOI:10.1142/S0218271824500160.

AUTHORS' INFORMATION

Suliyeva, Gulnara – PhD student, al-Farabi Kazakh National University, Almaty, Kazakhstan; Scopus Author ID: 57818572500; ORCID iD: 0000-0001-5072-7898; g_suliyeva@mail.ru

Kurmanov, Yergali – PhD, Acting Associate Professor, al-Farabi Kazakh National University, Leading Research Associate at the National Nanotechnology Open Laboratory (NNLOT), Almaty, Kazakhstan; Scopus Author ID: 57695578100; ORCID iD: 0000-0003-3695-0166; kurmanov.yergali@kaznu.kz

Konysbayev, Talgar – PhD, Senior Researcher, National Nanotechnology Open Laboratory (NNLOT), al-Farabi Kazakh National University, Almaty, Kazakhstan; Scopus Author ID: 5721980000; ORCID iD: 0000-0001-9476-3700; talgar_777@mail.ru

Boshkayev, Kuantay – PhD, Professor, al-Farabi Kazakh National University, Chief Researcher at the National Nanotechnology Open Laboratory (NNLOT), Almaty, Kazakhstan; Scopus Author ID: 54883880400; ORCID iD: 0000-0002-1385-270X; kuantay@mail.ru

Urazalina, Ainur – PhD, Senior Lecturer, al-Farabi Kazakh National University, Leading Research Associate at the National Nanotechnology Open Laboratory (NNLOT), Almaty, Kazakhstan; Scopus Author ID: 57076979300; ORCID iD:0000-0002-4633-9558; y.a.a.707@mail.ru

Luongo, Orlando – PhD, Associate Professor, University of Camerino, Camerino, Italy; Scopus Author ID: 35176257700; ORCID iD: 0000-0001-7909-3577; orlando.luongo@unicam.it